C. R. Chimie 21 (2018) 253–262

Contents lists available at ScienceDirect

Comptes Rendus Chimie

www.sciencedirect.com

Full paper/Mémoire

Efficient removal of cadmium and 2-chlorophenol in aqueous systems by natural clay: Adsorption and photo-Fenton degradation processes

Haithem Bel Hadjltaief [a], Ali Sdiri [a, *], Wahida Ltaief [a], Patrick Da Costa [b, **], María Elena Gálvez [b], Mourad Ben Zina [a]

[a] Laboratory of Water, Energy and Environment, National Engineering School, University of Sfax, Post Box 1173-3038, Sfax, Tunisia
[b] Institut Jean-Le-Rond-d'Alembert, Sorbonne Universités, UPMC University Paris-6, UMR CNRS 7190, 2, place de la Gare-de-Ceinture, 78210 Saint-Cyr-l'École, France

ARTICLE INFO

Article history:
Received 25 July 2016
Accepted 19 January 2017
Available online 28 February 2017

Keywords:
Photo-Fenton oxidation
Adsorption
Cadmium removal
2-Chlorophenol
Clays
Catalysis

ABSTRACT

Adsorption and photo-Fenton processes were used as handy tools to ascertain the capability of natural clays to remove cadmium (Cd) and 2-chlorophenol (2-CP) from aqueous solution. Natural Fe-rich clay collected from Tejera-Esghira in Medenine area, south Tunisia, was used as a catalyst in the heterogeneous photo-Fenton oxidation of 2-CP in aqueous solution. Clay samples were acid activated to improve their adsorptive capacity for the removal of Cd. Experimental results indicated that the adsorption of Cd ions onto natural red clay of Tejera-Esghira followed the pseudo-second-order kinetic model. Langmuir model was found to describe the equilibrium data with the calculated maximum adsorption capacity of 23.59 mg g^{-1} for acid-activated clay. Photo-Fenton experiments proved high activity of the natural clay catalyst, which was able to completely degrade the phenol present in the treated solution after 30 min and in the presence of ultraviolet light C (UV-C). Total organic carbon and gas chromatography analysis confirmed a 2-CP degradation mechanism toward an almost complete mineralization of the organic compound.

1. Introduction

Wastewater produced from process industry generally contains inorganic pollutants and other organic contaminants [1–4]. Heavy metals such as cadmium (Cd), copper, lead, chromium, and so forth along with phenol and its derivatives are hazardous pollutants generated in petroleum refinery [3,5]. The presence of these pollutants in the aquatic environment causes deleterious effects (i.e., chemical, physical, or biological threats). Moreover, the consumption of polluted water can cause detrimental effects on living organisms [3,7]. Cd and 2-chlorophenol (2-CP) are among the most harmful pollutants because of their detrimental effects to living organisms even at trace levels. The US Environmental Protection Agency imposes very severe regulations for Cd and 2-CP contents in wastewater; the maximum concentration should be less than 5 ppb for Cd(II) ions and 1 mg/L for 2-CP. Therefore, the removal of these pollutants from wastewater is needed to reduce the concentration of pollutants.

Several techniques used in the removal of Cd(II) from the wastewater include chemical precipitation, coagulation/flocculation, ion exchange, solvent extraction, cementation, complexation, electrochemical operations, biological operations, adsorption, evaporation, filtration,

* Corresponding author.
** Corresponding author.
E-mail addresses: ali.sdiri@enis.rnu.tn (A. Sdiri), patrick.da_costa@upmc.fr (P. Da Costa).

http://dx.doi.org/10.1016/j.crci.2017.01.009

and membrane processes [8]. Similarly, various methods such as distillation, liquid–liquid extraction, adsorption, pervaporation, and membrane extraction, thermal oxidation, catalytic oxidation, and photocatalytic degradation were used for the removal of 2-CP from aqueous solutions [9,10].

The choice of the treatment technique depends on various factors including efficiency of the process, operation, and costs. On the basis of these conditions, adsorption and photo-Fenton process are expected to have the required specifications for the removal of Cd and 2-CP in aqueous conditions.

Adsorption is one of the most commonly used processes because of its simple and convenient unit operation and for its low cost compared with other treatment processes. The use of adsorption contacting system for industrial and municipal wastewater treatment has become prevalent during recent years [11]. Adsorption is often used at the end of a treatment sequence for pollution control because of the high efficient purification. Activated carbon is recognized as an effective adsorbent because of its large surface area and high adsorption capacity. However, its high cost and difficult recovery from treated water limit its use as an adsorbent [12]. Numerous researchers including Sdiri et al. [13], Li et al. [14], Heidari et al. [15], and Eloussaief et al. [11] referred to several potential low cost adsorbents such as limestone, silicas, resins, clays, zeolites, and so forth.

Textural properties (e.g., low cost, high mechanical and chemical stability, availability, and ion exchange capability) confer good adsorption efficiencies to natural clays [11,16]. Tunisian Illitic, kaolinitic, and smectitic clays were used in the adsorption of volatile organic compound [17], heavy metals [11,16], and in the purification of industrial phosphoric acid [18].

Photo-Fenton or photo-assisted Fenton process has been reported as one of the fastest and most economical treatment processes. Using safe and environmentally benign reagents such as Fe^{2+} and H_2O_2, it produces •OH groups in the presence of irradiation with sunlight or an artificial light source [19]. The shortcomings of the homogeneous Fenton process reside in its requirement for high Fe concentration (between 50 and 80 ppm). This is well above the limits set by European Union directives, which allow a maximum of 2 ppm Fe in treated water to be discharged directly into the environment [19,20]. Therefore, the replacement of such a homogeneous catalyst by a heterogeneous system containing the active phase is needed. Different porous materials, including zeolites (synthetic and natural), clays, polymers, silica, carbon, or resins are among the best supports to disperse active phases [9,21,22]. Among these materials, clay minerals containing iron (i.e., pillared interlayered clays) are proposed as good candidates (as heterogeneous catalysts) for the oxidative degradation of organic compounds through the Fenton reaction [21,23]. The application of clay minerals as heterogeneous photo-Fenton catalysts is a very promising technology for the treatment of water containing organic pollutants because of the high surface areas, easy control, and high porosity [19]. In our previous works, iron-pillared Tunisian clays showed promising adsorption capacity and excellent photocatalytic ability for the removal of organic pollutants such as Congo red, Malachite green, and phenol in aqueous solution [19,20]. Natural Fe-rich clays could also be used as heterogeneous catalysts in the Fenton-like reaction. In fact, Tejera-Esghira Fe-rich clay is an ideal candidate that can be used as a Fenton catalyst because of the distribution of iron oxide species on the clay surface.

The application of natural clay as an adsorbent or as a Fenton catalyst is an attractive and innovative alternative because of the low cost and widely available material with high iron content, a key in the Fenton reaction mechanism. Those characteristics agree well with some of the “green chemistry” principles, such as the use of alternative feedstocks that are more innocuous and the design of ecocompatible chemicals [24]. In this context, this study has been undertaken to evaluate the potential use of natural Tunisian clay (RC) as natural adsorbent for Cd(II) and 2-CP removal in aqueous systems. Acid-activated natural red clay (AC) was also tested for the adsorption of Cd(II) ions in batch mode. The effect of metal ion concentration was investigated. Langmuir and Freundlich isotherms were used to analyze the equilibrium data. The natural red clay (i.e., RC) was used as heterogeneous photo-Fenton for the degradation of 2-CP from aqueous solution. The kinetics and mechanism of the degradation of 2-CP were considered as well.

2. Experimental section

2.1. Materials and chemicals

The RC used in this study was sampled in Jebel Tejera-Esghira deposits located in the Medenine district, Southeastern Tunisia (Fig. 1). From a geological point of view, those clays were attributed to the Lower Triassic, a very thick series with dominant sandstone alternating with red clays and some silty intercalations. The outcrops extended from the Beni Kheddache cliff to the J. Tebaga of Medenine; it occupies the anticline of the J. Tejera site. The outcropping feature of the Jebel Tajera-Esghira was estimated to be 80 m-thick deposits of ferruginous clays (Fig. 1).

The natural clay was first purified by dispersion in water, decantation, and extraction of the desired fraction ($\leq$2 μm-sized fraction) [24,25]. The cation exchange capacity of this material was 18.66 meq/100 g [6].

To enhance its textural properties (i.e., porosity, surface area, and so on), natural clay was also acid activated as follows: 10 g of powdered clay was suspended in 40 mL of distilled water. A solution of 6 M of H_2SO_4 was added dropwise at 7 °C under continuous stirring at 200 rpm for 4 h [2,17,26]. Then, the acid-treated clay was repeatedly washed to obtain a pH = 6. Finally, the obtained samples were dried at 60 °C and stored for further analyses.

2.2. Physicochemical characterization

Chemical composition and textural properties of both natural and activated clay were analyzed using X-ray fluorescence (ARL1 9800 XP spectrometer), powder X-ray diffraction (Philips1 PW 1710 diffractometer, Kα, 40 kV/40 mA, scanning rate of 2θ per minute). Specific surface

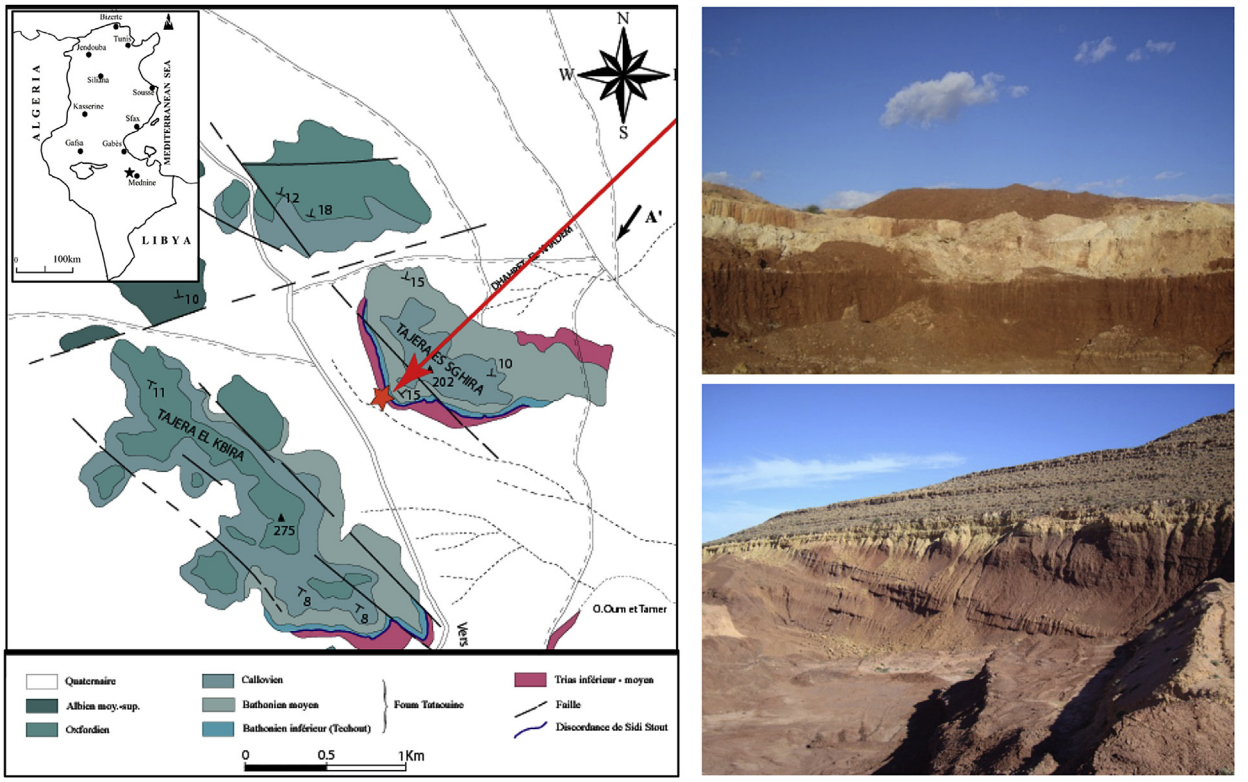

Fig. 1. Localization of the studied clay deposit. (Right panel) Outcroppings of the Triassic clays in Tejera-Esghira site.

area was measured by plotting nitrogen adsorption isotherms using a Micromeritics ASAP 2020 device. The structure and morphology of the samples were examined by scanning electronic microscopy (SEM; Hitachi SU-70) and high-resolution transmission electron microscopy (JEOL JEM 2011 equipped with LaB6 filament). The high-resolution transmission electron microscopy images were collected with a 4008 2672 pixel charge coupled device (CCD) camera (GatanOrius SC1000) coupled with the DIGITAL MICROGRAPH software. Coupled chemical analysis was obtained using an Emission Dispersive spectroscopy X (EDX) microanalyzer (PGT IMIX PC).

2.3. Adsorption and photo-Fenton studies

2.3.1. Batch adsorption study

Cd solutions were prepared by dilution of a 10 mM analytical grade standard solution of $CdCl_2$. Adsorption of Cd(II) onto activated clay was carried out using batch methodology under room temperature (20 °C) and pH = 7.0 [6].

The effect of contact time on the adsorption of Cd(II) was kinetically studied following the experimental procedure described by Sdiri et al. [16].

Adsorption isotherms were established by addition of a known amount of powdered clay (0.5 g) to 200 mL of Cd solution (concentrations, 20–400 mg/L) into 250 mL sealed Erlenmeyer flasks. The mixture was shaken at room temperature for 60 min to reach equilibrium. Then, the mixture was filtered and Cd(II) concentration was measured by atomic absorption spectrophotometry (ZEEnit 700 spectrometry, Analytik Jena). The adsorbed amounts of Cd(II) were calculated from the difference between initial and equilibrium concentrations as follows:

$$q_e = \frac{(C_0 - C_e)V}{m} \quad (1)$$

where q_e is the amount of Cd(II) ions adsorbed (mg/g), C_0 and C_e are initial and equilibrium Cd(II) concentrations (mg/L), respectively, V is the volume (L), and m is the adsorbent mass (g).

2.3.2. Photo-Fenton degradation studies

Photo-Fenton catalytic oxidation experiments were carried out in a 250-mL Pyrex open vessel, water-cooled, and placed on a magnetic stirrer under two parallel UV lamps 2–15 at 254 and 365 nm with 930/1350 mW cm^{-2}. The distance between the solution and the UV lamps was kept constant at 15 cm. All the experiments were performed at room temperature (i.e., 25 °C). After stabilization of the stirring speed (150 rpm), 0.5 g natural clay catalyst was added to 200 mL of an aqueous 2-CP solution ([2-CP] = 100 mg/L; pH = 3; prepared from analytical grade 99%, Merck). Then, 8 mL of H_2O_2 solution prepared at 1000 mg L^{-1} H_2O_2 standard solution (Merck reagent) was added to the reaction vessel. UV irradiation, H_2O_2, UV/H_2O_2, adsorption, and Fenton were carried at in the absence or in the presence of the natural clay (RC), as catalyst.

Aliquots were periodically withdrawn from the reaction vessel at predetermined time intervals (60 min of treatments). Residual H_2O_2 in these samples was, then, quenched with MnO_2 (99% Merck) to avoid the occurrence of a dark Fenton reaction through the possible presence of leached iron. Before analysis, the liquid was filtered using Polytétrafluoroéthène (PTFE) filters (0.45 μm).

The 2-CP concentration in the solution was analyzed by gas chromatography (GC), in an Agilent 2025 GC equipped with a Zebron capillary column ZB-5MSi (30 m × 0.32 mm × 0.25 μm) and a flame ionization detector. Total organic carbon (TOC) was measured using a TOC analyzer (TOC-5000A, Shimadzu, Japan) (catalytic oxidation on Pt at 680 °C) via calibration using standards of potassium phthalate.

Dissipation efficiency and mineralization efficiency were calculated as follows:

$$\text{Dissipation efficiency}: \quad \eta(\%) = ((C_0 - C_t)/C_0) \times 100$$

$$\text{Mineralization efficiency}: \quad \eta(\%) = ((\text{TOC}_0 - \text{TOC}_t)/\text{TOC}_0) \times 100$$

where C_0 and TOC_0 are the initial concentration and TOC of the 2-CP and C_t and TOC_t are the concentration and TOC of the 2-CP at the given reaction time (min), respectively.

The •OH concentration during the Fenton reaction was determined by a photometric method [27,28]. Free chloride ions were determined after each irradiation period using an ion chromatograph (HIC-6A Shimadzu, Japan) equipped with a conductivity detector and a Shim-pack column. The separation was achieved using an isocratic elution at a flow rate of 1.5 mL min^{-1}. A mobile phase of 1 mM of tris(hydroxymethyl)aminomethane and 1 g L^{-1} of sodium chloride was used as a standard solution.

3. Results and discussion

3.1. Characterization of adsorbent and catalyst materials

Chemical and physical characteristics of both natural (i.e., RC) and acid-activated clay (AC) are summarized in Table 1. The main constituents of the natural clay (RC) are silica, alumina, and iron oxides. High amount of iron was found in comparison (12.15 wt %) to other natural clays used in Fenton and photo-Fenton oxidation of phenol [3,4]. Acid activation decreased iron, calcium, and magnesium contents leading to the increased silica and alumina contents because of the effect of acid on carbonates [30]. On the other hand, acid-activated clay showed higher specific surface area, total pore volume, internal porosity, and pore size compared with untreated clay (Table 1).

Mineralogical analysis of the natural clay sample was identified by X-ray diffraction measurements [24,25]; it showed characteristic peaks of quartz (26.7), kaolinite (22.8), and illite (12.6). After calcination of the natural clay, iron oxide phases were observed in the form of α-Fe_2O_3 (about 64%), hematite, with diffraction peaks appearing at $2\theta = 32.2$, 35.7, and 36.4° [3,29].

The results for the temperature-programmed reduction for untreated and calcined clay are discussed in detail by Djeffal et al. [29]. The support reduction profiles showed only one reduction peak with shoulders near 470 °C; this can be assigned to superficial iron oxide (hematite; α-Fe_2O_3). Chemical and mineralogical analyses and temperature-programmed reduction profile indicated that Fe_2O_3 was the main iron species present in the studied clay samples, leading to higher oxidation activity of 2-CP.

SEM micrographs of RC and AC, presented in Fig. 2, were quite helpful for the clarification of the morphological change upon activation process. It was clearly observed that surface morphology of RC (Fig. 2a) was different from that of AC (Fig. 2b). Original clay sample showed larger particle aggregates with smooth surfaces, but after H_2SO_4 activation, the AC porous structure has been improved (Fig. 3).

3.2. Adsorption of Cd on AC

3.2.1. Kinetic models

The well-known pseudo-first-order and pseudo-second-order kinetic models were applied to the experimental data to examine the adsorption process.

The pseudo-first-order equation can be written as follows:

$$\frac{dq_t}{dt} = k_1(q_e - q_t) \tag{2}$$

where q_e and q_t are the adsorbed quantity (mg/g) at equilibrium and at time t, respectively; k_1 (min^{-1}) is the adsorption rate constant. The value of k_1 and q_e can be calculated from the slope and intercept of the linear plot of $\ln(q_e - q_t)$ versus t, respectively.

The pseudo-second-order kinetic model was also used to describe the sorption of metal ions. The differential equation for the reaction is expressed as:

$$\frac{dq_t}{dt} = k_2(q_e - q_t)^2 \tag{3}$$

Table 1
Chemical composition (% oxides, X-ray fluorescence), textural properties (V_p, pore volume, χ, porosity, and S_{BET}, surface area) of the natural red clay (RC) and acid-activated clay (AC).

	Chemical composition (%)								Textural properties		
	SiO_2	Al_2O_3	SO_3	K_2O	Cl	MgO	CaO	Fe_2O_3	V_p (cm^3/g)	χ (%)	S_{BET} (m^2/g))
RC	53.86	24.29	0.27	2.32	0.03	3.27	0.66	15.15	0.08	17	50
AC	61.50	27.00	0.01	1.13	0.02	0.74	0.05	1.74	0,19	25	90

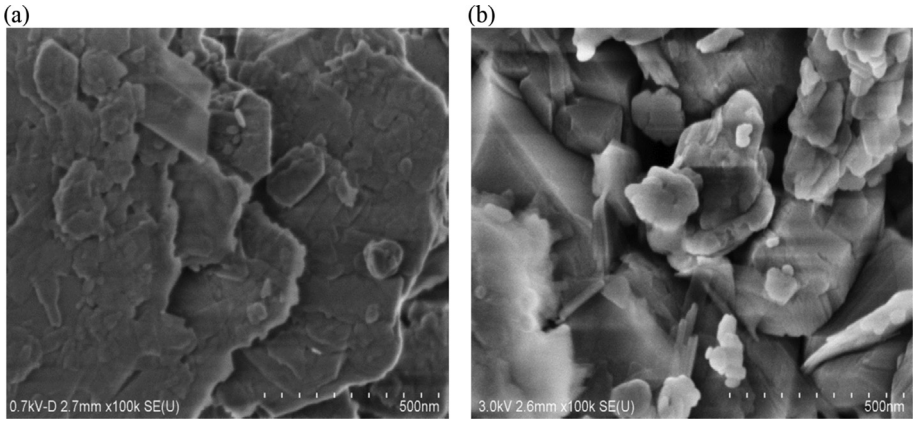

Fig. 2. SEM images of the natural red clay (a) and acid-activated clay (b).

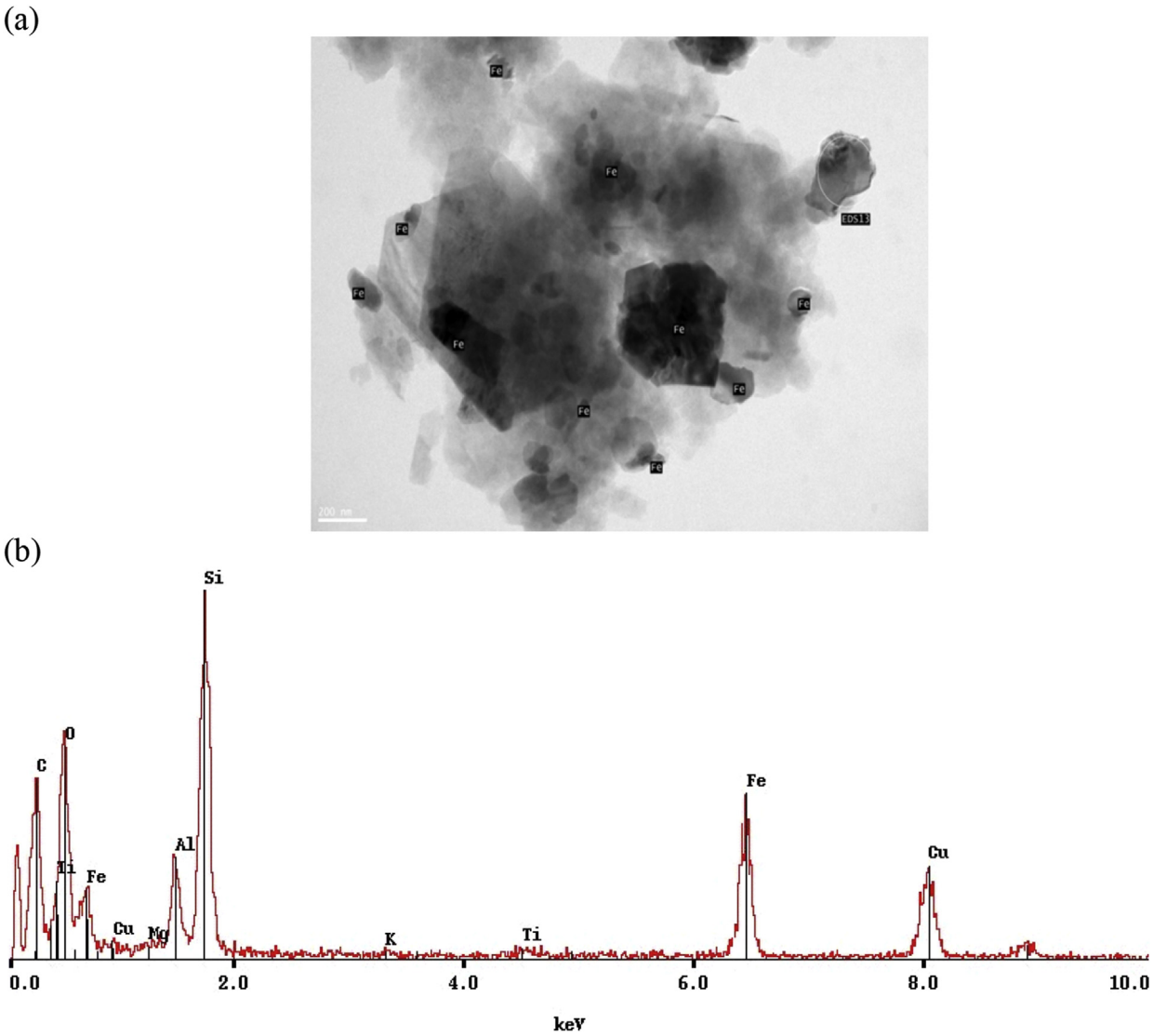

Fig. 3. (a) Transmission electron microscopy and (b) EDX elemental microanalysis of natural red clay.

k_2 is the pseudo-second-order rate constant (g mg^{-1} min^{-1}). Both constants, k_2 and q_e, were calculated from the intercept and slope of the linear plot t/qt against t, respectively.

The effect of contact time on the adsorption of Cd(II) onto AC was studied in the concentration range 20 −400 mg/L (Fig. 4). In the beginning, adsorption rate was higher because of the large number of reaction sites available, attained equilibrium within 20 min, but larger equilibrium time interval was considered. As the concentration of Cd(II) increases from 20 to 400 mg/L, the adsorption capacity obtained from experiments increases from 12.00 to 22.756 mg/g and theoretically calculated values (pseudo-first-order prediction) increase from 11.961 to 22.799 mg/g.

The adsorption of Cd onto activated clay sample showed good fittings to the pseudo-first-order model because of the similar values of experimentally measured and calculated amounts (Table 2).

The pseudo-second-order kinetic model was also used to describe the sorption process. Both constants, k_2 and q_e, were calculated from the intercept and slope of the linear plot t/q_t against t. The calculated and measured amounts of sorbed solute at equilibrium suggested that the process of Cd removal fitted both kinetic models (i.e., the pseudo-second-order kinetic model and the pseudo-first-order model; Table 2). Moreover, the coefficient of determination R^2 was high enough to opt for the pseudo-first-order model. This result contradicted those found by Sari et al. [31] and Sdiri et al. [13,16] who studied the removal of several metal ions from aqueous solutions by natural geological materials (i.e., kaolinite clay [31] and smectitic clay [13,16]).

3.2.2. Adsorption isotherms

Langmuir model assumes that adsorption occurs at specific homogeneous sites on the surface of the adsorbent. When a site is occupied by an adsorbate molecule, no further adsorption can occur at this site [16]. The Langmuir isotherm model can be expressed by the following relationship:

$$q_e = \frac{q_{max} K_L C_e}{1 + K_L C_e} \quad (4)$$

where q_e (mg/g) is the amount of Cd adsorbed onto the AC at equilibrium, q_{max} (mg/g) is the theoretical monolayer capacity, K_L is the Langmuir equilibrium constant, which is related to the affinity of binding sites and the energy of adsorption, and C_e (mg/L) is the concentration of the equilibrium solution.

Freundlich isotherm model is an empirical equation, and the model is valid for adsorption that occurs on heterogeneous surfaces [32]. Freundlich isotherm equation is expressed as:

$$q_e = K_F C_e^{1/n} \quad (5)$$

where K_F (L mg^{-1}) and n are the Freundlich constants associated with the relative capacity and adsorption intensity, respectively.

Fig. 5 shows the adsorption isotherm of Cd(II) onto AC at 293 K and pH = 7. It presents a straightforward relationship between the amount of adsorbed Cd(II) per unit mass of clay (q_e) versus equilibrium concentration (C_e). Calculated parameters for both Langmuir and Freundlich isotherms are listed in Table 3. It was clearly observed that adsorbed amount given by Langmuir isotherm fitted well the experimental data ($R^2 = 0.99$); this was comparable to that

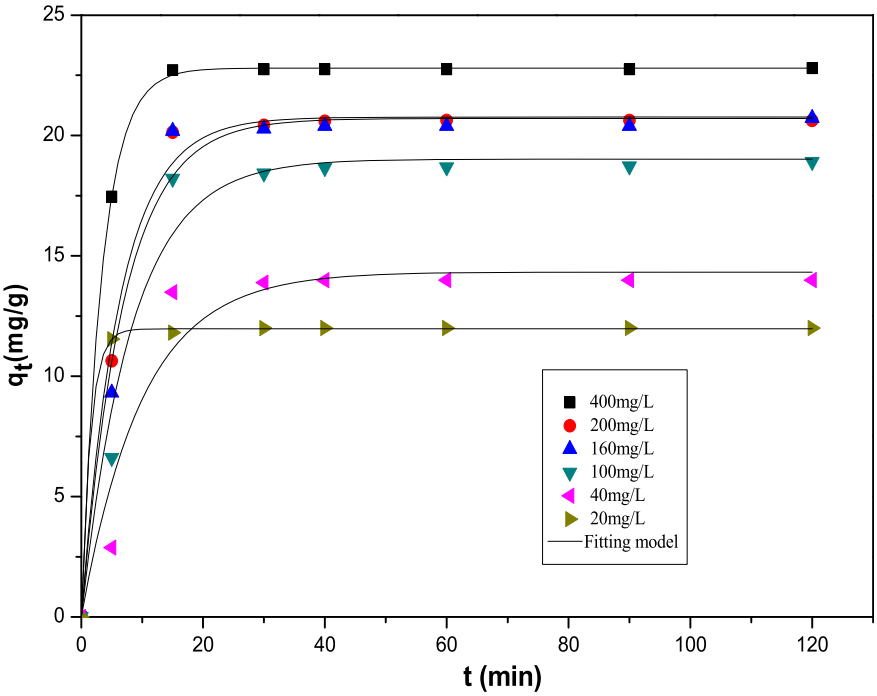

Fig. 4. Adsorption kinetics of Cd(II) onto red clay at different concentrations.

Table 2
Kinetic parameters for the adsorption of Cd(II) onto acid-activated clay (AC).

Initial concentration (mg/L)	q_e measured (mg/g)	Pseudo-first-order			Pseudo-second-order		
		q_e (mg/g)	k_1 (min^{-1})	R^2	q_e (mg/g)	k_2 (g mg^{-1} min^{-1})	R^2
400	22.756	22.799	0.291	0.999	22.896	0.1	0.9999
200	20.622	20.767	0.1590	0.993	20.959	0.033	0.9988
160	20.397	20.707	0.1436	0.984	21.036	0.024	0.9979
100	18.683	19.020	0.1207	0.97	19.452	0.018	0.9951
40	13.994	14.328	0.099	0.93	14.927	0.012	0.9762
20	12.000	11.961	0.665	0.999	12.014	0.77	0.9999

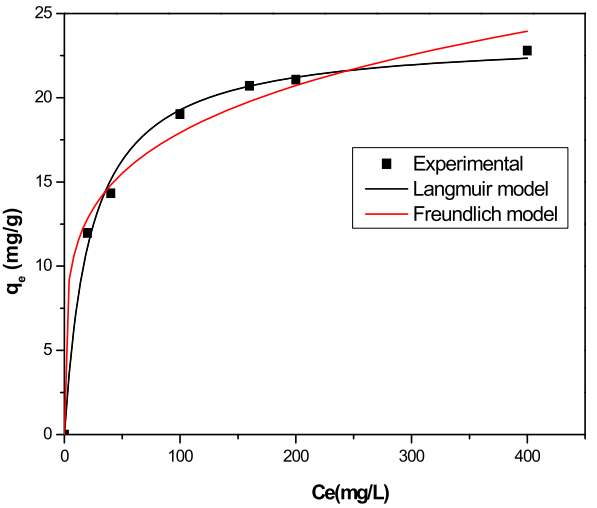

Fig. 5. Comparison of different isotherm models for Cd(II) adsorption onto red clay.

obtained from Freundlich isotherm ($R^2 = 0.98$). Therefore, both Langmuir and Freundlich isotherms fitted the adsorption of Cd onto the activated clay, with somewhat higher coefficient of determination for Langmuir. Thus, we adopted Langmuir isotherm for the description of the removal process. Maximum adsorption capacity of Cd(II) was 23.593 mg/g, which was higher than that of carbon nanotubes (14.45 mg/g [33]), porous resins (3.51 mg/g [14]), mesoporous silica materials (18.25 mg/g [15]), clay materials such as kaolinite (6.80 mg/g [34]), vermiculite (20.7 mg/g [35]) but lower than smectitic clay (26.7 mg/g [36]) and activated sericite (39.83 mg/g [37]).

3.3. Photo-Fenton degradation over natural RC

3.3.1. Catalytic performance of RC in the photo-Fenton oxidation of 2-CP

2-CP was used as a model pollutant to investigate the catalytic activity of natural clay under different conditions at the initial solution pH = 3.0. As shown in Fig. 6a, 2-CP was scarcely degraded in the presence of UV irradiation of 254 nm wavelength or H_2O_2 separately, indicating that the degradation of 2-CP was very limited [38]. In the presence of natural RC , maximum 2-CP reduction around 22.1% was measured; it stabilizes after 30 min of reaction time. This 2-CP decrease can be ascribed to its adsorption on the clay surface (corresponding to an adsorption capacity of around 28.6 mg of 2-CP per gram of the catalyst), although 2-CP oxidation in the presence of this catalyst might not be neglected. After 60 min of treatment, 61.72% of 2-CP was degraded because of the direct photolysis of H_2O_2 under UVC irradiation. The 2-CP degradation was significantly enhanced in the presence of natural clay and H_2O_2, indicating the catalyst acts as a Fenton catalyst. The oxidation reaction may be hindered to some extent by the presence of originally inactive Fe species like Hematite form (α-Fe_2O_3) [25,38]. UV irradiation is an important key for achieving higher 2-CP removal efficiencies [25]. When reaction is performed in the presence of RC and H_2O_2 under UVC irradiation, 100% 2-CP removal can be finally attained. This fact proved higher effectiveness of the photo-Fenton process compared with dark Fenton reaction, which was because of the enhanced formation of radicals [25,29,38]. Those results confirmed that RC exhibited good catalytic activity for Fenton and photo-Fenton reactions. As shown in Fig. 6b, ln (C_0/C) was highly linear versus reaction time within 30 min. The degradation of 2-CP followed pseudo-first-order kinetics over RC in the presence of H_2O_2 under UVC irradiation. The reaction rate constant (k) was 0.0123 and 0.0524 min^{-1} for Fenton and photo-Fenton processes, respectively.

Compared with Fenton reaction, higher efficiency for 2-CP degradation in the photo-Fenton process may be attributed to the regeneration of Fe^{2+} by UV irradiation. To confirm this hypothesis, formation of chloride ions and production of •OH in Fenton and photo-Fenton processes were determined (Fig. 7). It was clearly observed that chloride ions increased with reaction time. Such a behavior was expected because of the higher efficiency in the photo-Fenton reaction than that in the Fenton reaction. Correspondingly, the •OH formation rate in the photo-Fenton process was about six times higher than that in the Fenton process, indicating a good catalytic activity of the photo-Fenton process and better •OH generation; it resulted in a stronger oxidation ability for the degradation of 2-CP.

Table 3
Isotherm parameters for the adsorption of Cd(II) onto acid-activated clay (AC).

Adsorbent	Langmuir			Freundlich		
	q_{max} (mg/g)	K_L (L mg^{-1})	R^2	K_F (L g^{-1})	n	R^2
	23.593	0.0445	0.99	6.854	4.790	0.98

3.3.2. Intermediate 2-CP

It is well known that the complete oxidation (i.e., mineralization) of 2-CP occurs through the formation of

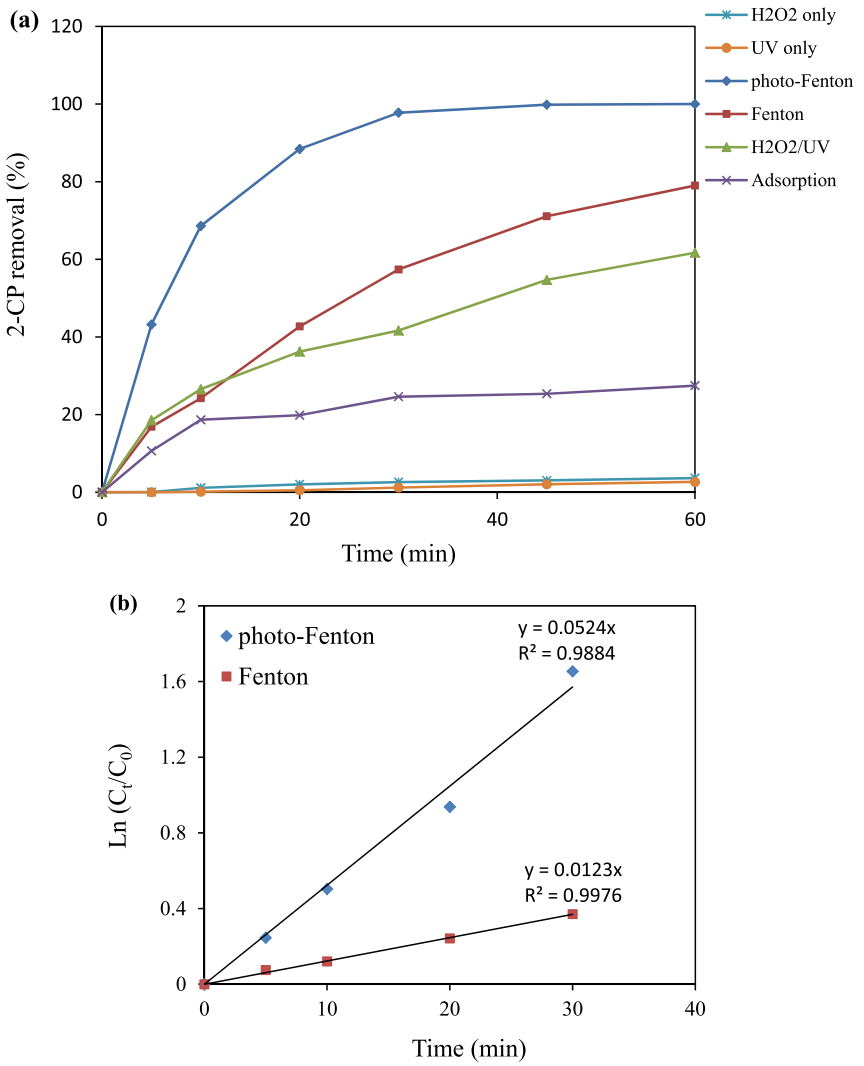

Fig. 6. (a) Degradation of 2-CP at different experimental conditions; (b) 2-CP degradation kinetics during the Fenton and photo-Fenton processes ($[2\text{-CP}]_0$ = 100 mg/L, red clay dosage = 0.5 g L^{-1}, 8 mL of H_2O_2, $[H_2O_2]$ = 1000 mg/L, pH = 3.0).

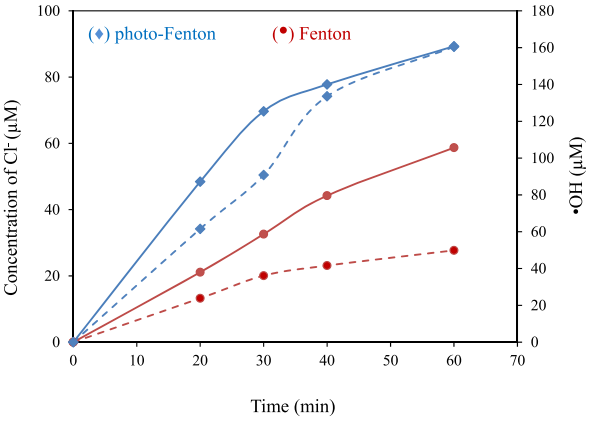

Fig. 7. Chloride ions and •OH formation during Fenton and photo-Fenton processes with red clay catalyst ($[2\text{-CP}]_0$ = 100 mg/L, red clay dosage = 0.5 g L^{-1}, 8 mL of H_2O_2, $[H_2O_2]$ = 1000 mg/L, pH = 3.0).

several intermediate reactions, such as benzoquinone, hydroxybenzoquinone (yellow), and hydroquinone (colorless) and/or maleic and other carboxylic acids, some of them being even more toxic than 2-CP itself [10]. Fig. 8 shows the suggested mechanism of 2-CP photo-Fenton oxidation: the first step of the irradiation process removed the chlorine atom from 2-CP, after which hydroxyl radicals attack the compound to generate hydroquinone. Hydroquinone molecules are subsequently dehydrogenated to benzoquinone. The availability of excess hydroxyl radicals breaks the benzoquinone ring to produce aliphatic carboxylic acids, such as maleic and fumaric acids. Further oxidation of maleic acid produces oxalic acid whose oxidization produces formic acid and, finally, carbon dioxide. This proposed pathway is similar to other chlorophenolic substrate decomposition reaction pathways [10,39,40].

The mineralization of the process was monitored by TOC measurements and GC. Table 4 shows the results of 2-CP

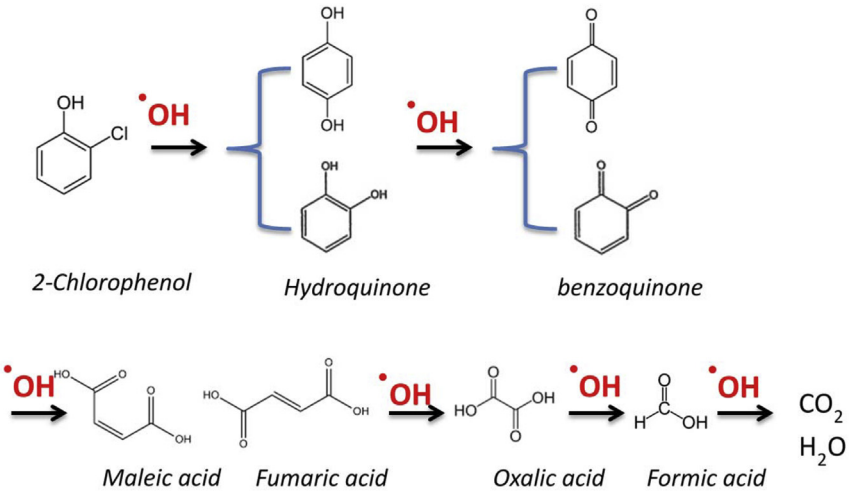

Fig. 8. A proposed reaction pathway of 2-CP degradation involving hydroxyl radicals.

Table 4
2-CP removal and mineralization efficiency measured during experimental runs under different reaction conditions at 60 min of treatment ($[2\text{-CP}]_0$ = 100 mg/L, red clay dosage = 0.5 g L^{-1}, 8 mL of H_2O_2, $[H_2O_2]$ = 1000 mg/L, pH = 3.0).

Process	2-CP removal (%)	2-CP mineralization (%)
H_2O_2 only	3.66	1.01
UV only	5.35	1.36
Adsorption	27.45	15.26
UV/H_2O_2	61.72	43.62
Fenton	81.01	55.3
Photo-Fenton	100	100

mineralization, measured by means of TOC analyses, for the same reaction conditions as those depicted in Fig. 6. These results evidence first that 2-CP cannot be mineralized in the sole presence of UVC irradiation, H_2O_2, or the catalyst. Mineralization is clearly enhanced in the photolysis of H_2O_2 or the Fenton process. Total mineralization of 2-CP can be obtained after 60 min of reaction in the presence of the RC catalyst, H_2O_2, and UVC irradiation. In addition, Fig. 9 shows the gas chromatograms acquired for aliquots taken out of the reaction vessel at different reaction times, during 2-CP degradation experiment upon H_2O_2 addition in the presence of the RC catalyst and UV irradiation of 254 nm wavelength. 2-CP peak appears at a retention time of 3.75 min. The intensity of this 2-CP peak decreases,

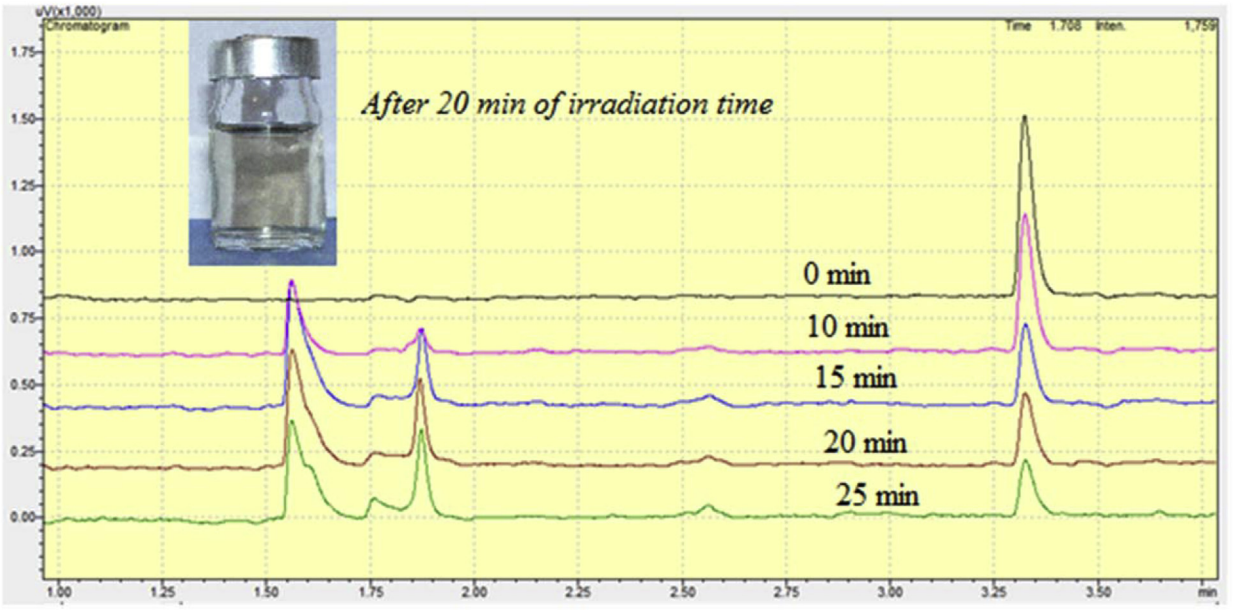

Fig. 9. Gas chromatograms for the solutions extracted from the reaction vessel at different reaction times, during the photo-Fenton 2-CP removal experiment in the presence of the red clay upon H_2O_2 addition and UV_{254} irradiation, together with the picture taken from final solution.

whereas the intensity of the peak appearing at retention times immediately near to that of 2-CP increases in the range retention time between 1.75 and 2.75 min. After treatment (25 min of reaction), the solution shows a certain brownish color during degradation of the 2-CP and may point to the presence of *p*-benzoquinone and/or *o*-benzoquinone intermediates [25]. After 120 min of irradiation, the concentration of these major intermediates dropped sharply, indicating the mineralization of 2-CP [25].

4. Conclusions

Clay samples of the Late Triassic, southern Tunisia, were mainly composed of ferrous aluminosilicates with substantial amounts of kaolinite and illite. The original and treated clay samples were used for the removal of Cd and 2-CP from aqueous solution. From the adsorption study, it was concluded that both clays can effectively remove Cd cations (Cd(II)) in aqueous conditions.

Our study showed that good adsorptive capacities could be achieved under the following operating conditions: 60 min of contact time, pH = 7, and clay concentration of 2 g L^{-1}. The experimental data demonstrated a high degree of fitness to the pseudo-second-order kinetics and Langmuir model. Photo-Fenton process has also been used as a facile technique for the aquatic degradation of organic pollutants. 2-CP was used as a model pollutant to investigate the catalytic activity of natural clay under different conditions. It was found that photo-Fenton process showed high effectiveness of 2-CP degradation when compared with a dark Fenton reaction. These results confirmed good catalytic activities for Fenton and photo-Fenton reactions.

It is therefore plausible to affirm that the iron-rich clays from southern Tunisia are promising natural resources that can effectively remove both organic and inorganic pollutants in aqueous conditions.

References

[1] A.T. Sdiri, T. Higashi, F. Jamoussi, Int. J. Environ. Sci. Technol. 11 (2014) 1081–1092, http://dx.doi.org/10.1007/s13762-013-0305-1.
[2] M. Eloussaief, M. Benzina, J. Hazard. Mater. 178 (2010) 753–757.
[3] H. Bel Hadjltaief, P. Da Costa, P. Beaunier, M.E. Gálvez, M. Ben Zina, Appl. Clay Sci. 91–92 (2014) 46–54, http://dx.doi.org/10.1016/j.clay.2014.01.020.
[4] L. Djeffal, S. Abderrahmane, M. Benzina, M. Fourmentin, S. Siffert, S. Fourmentin, Environ. Sci. Pollut. Res. Int. (2013) 3331–3338, http://dx.doi.org/10.1007/s11356-013-2278-5.
[5] I. Bel Hadj Ali, Z. Lafhaj, M. Bouassida, I. Said, Int. J. Sediment Res. 29 (2014) 391–401, http://dx.doi.org/10.1016/S1001-6279(14)60053-6.
[6] I. Ghorbel-Abid, K. Galai, M. Trabelsi-Ayadi, Desalination 256 (2010) 190–195, http://dx.doi.org/10.1016/j.desal.2009.06.079.
[7] F. Shahriari, T. Higashi, K. Tamura, Soil Sci. Plant Nutr. 56 (2010) 560–569, http://dx.doi.org/10.1111/j.1747-0765.2010.00491.x.
[8] M. Khairy, S.A. El-Safty, M.A. Shenashen, TrAC Trends Anal. Chem. 62 (2014) 56–68, http://dx.doi.org/10.1016/j.trac.2014.06.013.
[9] L.F. Liotta, M. Gruttadauria, G. Di Carlo, G. Perrini, V. Librando, J. Hazard. Mater. 162 (2009) 588–606, http://dx.doi.org/10.1016/j.jhazmat.2008.05.115.
[10] M. Vallejo, P. Fernández-Castro, M.F. San Román, I. Ortiz, Chemosphere 137 (2015) 135–141, http://dx.doi.org/10.1016/j.chemosphere.2015.06.056.
[11] M. Eloussaief, A. Sdiri, M. Benzina, Environ. Sci. Pollut. Res. 20 (2013) 469–479.
[12] E.I. Unuabonah, K.O. Adebowale, F.A. Dawodu, J. Hazard. Mater. 157 (2008) 397–409, http://dx.doi.org/10.1016/j.jhazmat.2008.01.047.
[13] A. Sdiri, T. Higashi, F. Jamoussi, S. Bouaziz, T. Hatta, F. Jamoussi, N. Tase, S. Bouaziz, J. Environ. Manage. 93 (2012) 171–179, http://dx.doi.org/10.1016/j.jenvman.2011.08.002.
[14] C. Li, H. Duan, X. Wang, X. Meng, D. Qin, Chem. Eng. J. 262 (2015) 250–259, http://dx.doi.org/10.1016/j.cej.2014.09.105.
[15] A. Heidari, H. Younesi, Z. Mehraban, Chem. Eng. J. 153 (2009) 70–79, http://dx.doi.org/10.1016/j.cej.2009.06.016.
[16] A. Sdiri, T. Higashi, T. Hatta, F. Jamoussi, N. Tase, Chem. Eng. J. 172 (2011) 37–46, http://dx.doi.org/10.1016/j.cej.2011.05.015.
[17] M. Eloussaief, I. Jarraya, M. Benzina, Appl. Clay Sci. 46 (2009) 409–413.
[18] W. Hamza, C. Chtara, M. Benzina, Environ. Sci. Pollut. Res. 23 (2016) 15820–15831.
[19] H. Bel Hadjltaief, M. Benzina, M.E. Galvez, P. Da Costa, C. R. Chim. 18 (2015) 1161–1169, http://dx.doi.org/10.1016/j.crci.2015.08.004.
[20] H. Bel Hadjltaief, P. Da Costa, M.E. Galvez, M. Ben Zina, Ind. Eng. Chem. Res. 52 (2013) 16656–16665.
[21] E.G. Garrido-Ramírez, B.K. Theng, M.L. Mora, Appl. Clay Sci. 47 (2010) 182–192, http://dx.doi.org/10.1016/j.clay.2009.11.044.
[22] S. Navalon, M. Alvaro, H. Garcia, Appl. Catal. B Environ. 99 (2010) 1–26, http://dx.doi.org/10.1016/j.apcatb.2010.07.006.
[23] J.H. Ramirez, C.A. Costa, L.M. Madeira, G. Mata, M.A. Vicente, M.L. Rojas-Cervantes, A.J. López-Peinado, R.M. Martín-Aranda, Appl. Catal. B Environ. 71 (2007) 44–56, http://dx.doi.org/10.1016/j.apcatb.2006.08.012.
[24] H. Bel Hadjltaief, M. Ben Zina, M.E. Galvez, P. Da Costa, J. Photochem. Photobiol. A Chem. 315 (2016) 25–33, http://dx.doi.org/10.1016/j.jphotochem.2015.09.008.
[25] H. Bel Hadjltaief, M.E. Galvez, M. Ben Zina, P. Da Costa, Arab. J. Chem. (2014), http://dx.doi.org/10.1016/j.arabjc.2014.11.006.
[26] M. Eloussaief, N. Kallel, A. Yaacoubi, M. Benzina, Chem. Eng. J. 168 (2011) 1024–1031.
[27] C. Babbs, M. Gale, Anal. Biochem. 163 (1) (1987) 67–73.
[28] T.A. Ruda, P.K. Dutta, Environ. Sci. Technol. 39 (2005) 6147–6152, http://dx.doi.org/10.1021/es050336e.
[29] L. Djeffal, S. Abderrahmane, M. Benzina, S. Siffert, S. Fourmentin, Desalin. Water Treat. 52 (2014) 2225–2230, http://dx.doi.org/10.1080/19443994.2013.799440.
[30] A. Sdiri, T. Higashi, T. Hatta, F. Jamoussi, N. Tase, Environ. Earth Sci. 61 (2010) 1275–1287, http://dx.doi.org/10.1007/s12665-010-0450-5.
[31] A. Sari, M. Tuzen, D. Citak, M. Soylak, J. Hazard. Mater. 149 (2007) 283–291.
[32] H.M.F. Freundlich, J. Phys. Chem. 57 (1906) 385–470.
[33] W. Sun, B. Jiang, F. Wang, N. Xu, Chem. Eng. J. 264 (2015) 645–653, http://dx.doi.org/10.1016/j.cej.2014.11.137.
[34] S.S. Gupta, K.G. Bhattacharyya, J. Hazard. Mater. 128 (2006) 247–257.
[35] E. Padilla-Ortega, R. Leyva-Ramos, J. Mendoza-Barron, Appl. Clay Sci. 88–89 (2014) 10–17, http://dx.doi.org/10.1016/j.clay.2013.12.012.
[36] L. Khalfa, M. Bagane, J. Encapsulation Adsorpt. Sci. 1 (2011) 65–71, http://dx.doi.org/10.4236/jeas.2011.14009.
[37] L. Siama, D. Tiwari, S.-M. Lee, Chem. Eng. J. 283 (2016) 1414–1423, http://dx.doi.org/10.1016/j.cej.2015.08.072.
[38] E. Martin del Campo, R. Romero, G. Roa, E. Peralta-Reyes, J. Espino-Valencia, R. Natividad, Fuel 138 (2014) 149–155, http://dx.doi.org/10.1016/j.fuel.2014.06.014.
[39] L. Zhang, L. Lyu, Y. Nie, C. Hu, Sep. Purif. Technol. 157 (2016) 203–208, http://dx.doi.org/10.1016/j.seppur.2015.11.021.
[40] G.S. Pozan, A. Kambur, Chemosphere 105 (2014) 152–159, http://dx.doi.org/10.1016/j.chemosphere.2014.01.022.